MICROCOPY RESOLUTION TEST CHART
NATIONAL BUREAU OF STANDARDS-1963-A

AFGL-TR-84-0077

APPLICATION OF THE DIRECT SIMULATION MONTE
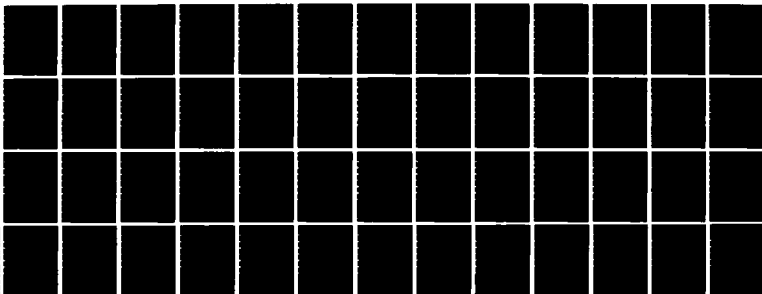CARLO METHOD TO MASS SPECTROMETER FLOW

James B. Elgin

Spectral Sciences, Inc.
111 So. Bedford Street
Burlington, MA   01803

Scientific Report No. 2

February 1984

AIR FORCE GEOPHYSICS LABORATORY
AIR FORCE SYSTEMS COMMAND
UNITED STATES AIR FORCE
HANSCOM AFB, MASSACHUSETTS 01731

AD-A142 326

DTIC FILE COPY

JUN 2 2 1934

A

84   06   22   011

This report has been reviewed by the ESD Public Affairs Office (PA) and is releasable to the National Technical Information Service (NTIS).

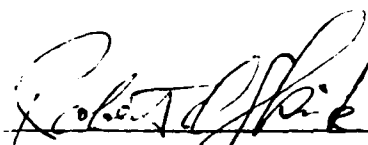This technical report has been reviewed and is approved for publication

CHRISTOPHER SHERMAN
Contract Manager

ROCCO S. NARCISI
Branch Chief

FOR THE COMMANDER

ROBERT A. SKRIVANEK
Division Director (Acting)

Qualified requestors may obtain additional copies from the Defense Technical Information Center. All others should apply to the National Technical Information Service.

If your address has changed, or if you wish to be removed from the mailing list, or if the addressee is no longer employed by your organization, please notify AFGL/DAA, Hanscom AFB, MA 01731. This will assist us in maintaining a current mailing list.

Do not return copies of this report unless contractual obligations or notices on a specific document requires that it be returned.
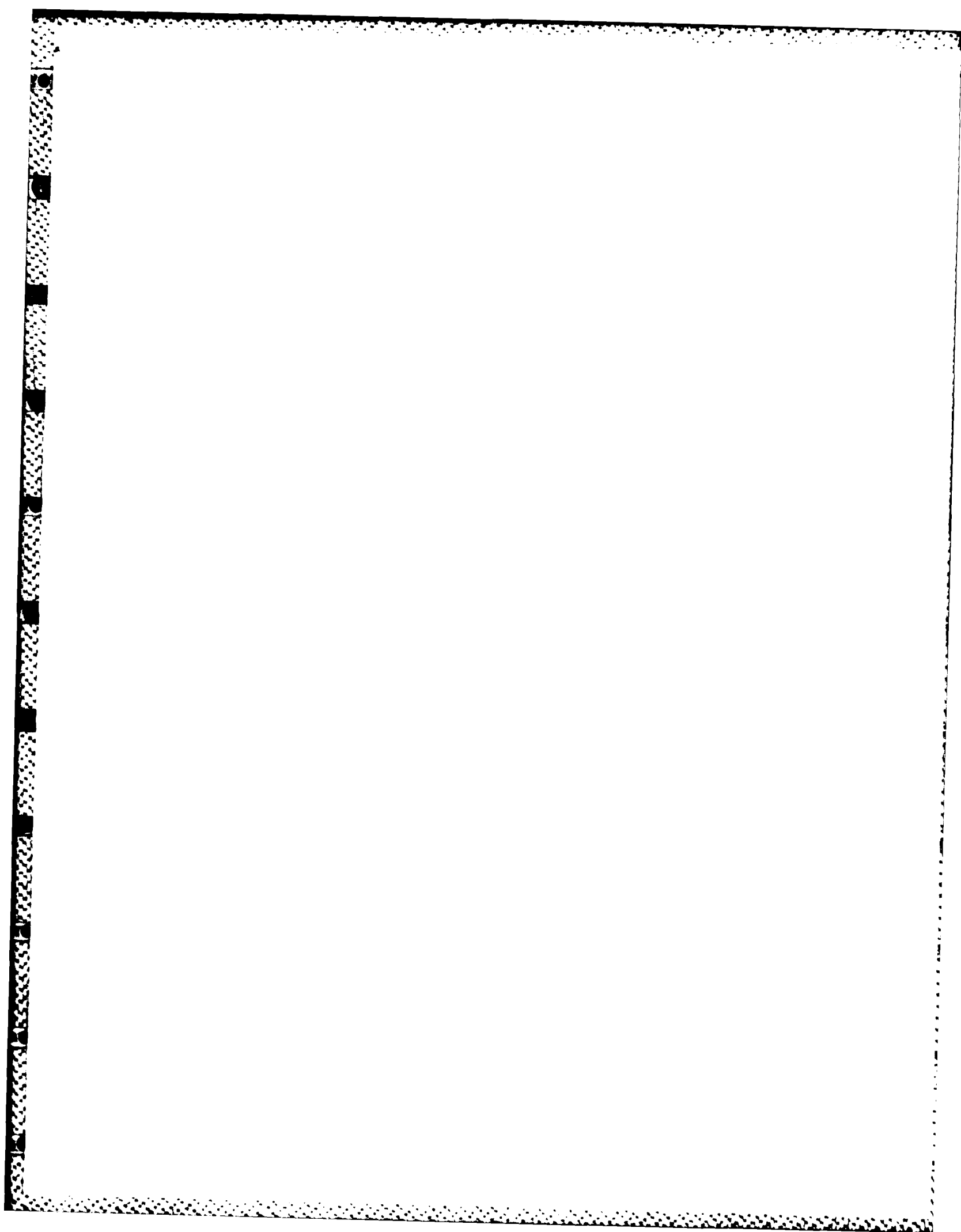
SECURITY CLASSIFICATION OF THIS PAGE (When Data Entered)

REPORT DOCUMENTATION PAGE		READ INSTRUCTIONS BEFORE COMPLETING FORM
1. REPORT NUMBER AFGL-TR-84-0077	2. GOVT ACCESSION NO. AD.A142 326	3. RECIPIENT'S CATALOG NUMBER
4. TITLE (and Subtitle) APPLICATION OF THE DIRECT SIMULATION MONTE CARLO METHOD TO MASS SPECTROMETER FLOW		5. TYPE OF REPORT & PERIOD COVERED Scientific Report No. 2 26 Jan. 83 – 26 Jan. 84
		6. PERFORMING ORG. REPORT NUMBER SSI-TR-45
7. AUTHOR(s) James B. Elgin		8. CONTRACT OR GRANT NUMBER(s) F19628-82-C-0048
9. PERFORMING ORGANIZATION NAME AND ADDRESS Spectral Sciences, Inc. 111 So. Bedford Street Burlington, MA 01803		10. PROGRAM ELEMENT, PROJECT, TASK AREA & WORK UNIT NUMBERS 62101F 668703AQ
11. CONTROLLING OFFICE NAME AND ADDRESS Air Force Geophysics Laboratory Hanscom AFB, MA 01731 Monitor/Christopher Sherman/LKD		12. REPORT DATE February 1984
		13. NUMBER OF PAGES 53
14. MONITORING AGENCY NAME & ADDRESS(If different from Controlling Office)		15. SECURITY CLASS. (of this report) UNCLASSIFIED
		15a. DECLASSIFICATION/DOWNGRADING SCHEDULE

16. DISTRIBUTION STATEMENT (of this Report)

Approved for public release; distribution unlimited.

17. DISTRIBUTION STATEMENT (of the abstract entered in Block 20, if different from Report)

18. SUPPLEMENTARY NOTES

19. KEY WORDS (Continue on reverse side if necessary and identify by block number)

Mass Spectrometer   Monte Carlo Flowfield

Freejet Expansion   Ionic Sampling

20. ABSTRACT (Continue on reverse side if necessary and identify by block number)

Technical progress is described in the development of a Monte Carlo code to simulate the flow within a mass spectrometer used to sample stratospheric ion clusters. A procedure is presented for spatially segmenting the solution region and a new formulation of the molecular internal energy model is described in terms of a Chi-Square distribution function.

DD FORM 1473 EDITION OF 1 NOV 65 IS OBSOLETE
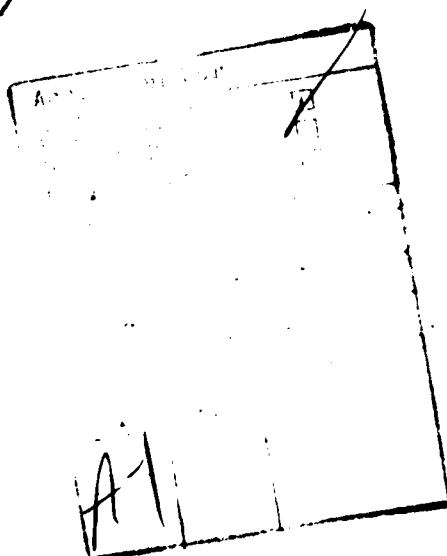1 JAN 73

S/N 0102-LF-014-6601

20. ABSTRACT (continued)

The modeling of accelerations due to electric fields is discussed and a comparison with published data for diffusive species separation is made.

CONTENTS

Contents (Continued)

ILLUSTRATIONS

1. INTRODUCTION

This is the second yearly technical report on a three year
effort to study physical processes of relevance to the mass
spectrometric measurement of stratospheric ions. The effort
involves the development of a Monte Carlo model of the free jet
expansion occurring within the mass spectrometer including the
effects of agglomeration onto, and fragmentation of, ionic
clusters.

The attempt to carry out in situ mass spectrometry in the
stratosphere is complicated by changes that may occur in the gas
stream as it expands after passage through the orifice. Both
positive and negative ions exist in the stratosphere with clus-
tered polar molecules surrounding the ion core. As these ion
clusters are carried along in the expanding gas stream, the
falling temperature will tend to favor the formation of larger
clusters. The charge-dipole interaction is characterized by
large cross sections, so agglomeration of polar molecules may
change the cluster size distribution that the quadrupole sees
from the distribution that exists in the undisturbed stratos-
phere. Conversely, the measured cluster size distribution may
be driven towards smaller clusters via fragmentation. As the
ionic clusters are selectively accelerated by the electric field
within the mass spectrometer, high energy collisions with neutrals
may break apart the clusters.

The present effort involves a Monte Carlo simulation of
these processes, so that a model can be used to relate the
measured properties to those existing in the undisturbed atmos-
phere. The basic elements of the direct simulation Monte Carlo
method were described in the previous yearly report,[1] and they

---

[1] Elgin, J. B., "Monte Carlo Calculations of Mass Spectrometer
Flow," Report AFGL-TR-83-0057, Air Force Geophysics Laboratory,
February 1983. ADA 128069.

will not be repeated here. There were substantial advancements made in the past year which are described in detail in this report. Section 2 describes the ability to treat separa.e spatial segments of the flowfield in separate computer runs, providing a substantial increase in computational efficiency. The formalisms for handling the simulation of internal molecular energy and its interchange with the translational mode have been generalized in terms of the classic Chi-Square distribution, and this generalization is discussed in Section 3. Means of efficiently sampling from a Chi-Square distribution were developed, and are discussed in Section 4.

The final new development for the past year is the inclusion of the accelerating effect of electric fields on charged species, and this item is discussed in Section 5. Section 6 presents a summary of the code status and Section 7 discusses a test case calculating the diffusive separation of a binary mixture of CO_2 and H_2.

2. SPATIAL SEGMENTATION OF SOLUTION REGION

The code was generalized in the past year so that it has the ability to compute sequential spatial segments of the solution starting from the orifice. (This new ability is merely an option and in no way affects the capability of handling the entire flow field at once.) The use of this option offers the potential for a substantial decrease in the memory and computing time required to solve a problem. Details of the spatial segmentation scheme are discussed in the subsections below.

2.1 Justification for Segmentation

The first question that must be addressed is whether the segmentation of the solution is physically and mathematically

justified, and this question is critically related to the question of boundary conditions. The physical laws that are embodied in the Monte Carlo solution procedure, involving molecular translations and collisions, are as valid for a portion of the solution region as they are for the whole region. In order to carry out the solution in just a subregion, however, it is necessary that the boundary conditions can be specified a priori alone 'e boundaries of the subregion in question.

For a Monte Carlo flow field calculation, the bou ary conditions are imposed by specifying the velocity dist. i' .tion function for incoming molecules alone all boundaries, and then selecting molecules from this distribution with the proper frequecy and introducing them into the simulation. Usually this involves extending the boundaries to a region of undisturbed (known) flow, or to a region where molecular backflow into the solution region is insignificant.

In the simulation of mass spectrometer flow, the upstream boundary is taken to correspond to one dimensional sonic conditions at the orifice, except that the mass flow is reduced by an empirically determined discharge coefficient. The solution region is extended far enough downstream and to the side so that the flow of molecules into the solution region from these other boundaries can be neglected. (An exception to this is the incursion of background gas into the jet which will be treated as an equilibrium gas at the side boundaries. This feature has not yet been added to the code, but it does not affect the present discussion since the distribution function for this gas will be assumed known at the side boundaries.) Hence, a well defined solution can be carried out downstream of the orifice as long as the downstream boundary is far enough from the orifice to assure that molecular backflow is negligible. Since molecules have a

thermal velocity which is on the order of the speed of sound, backflow becomes negligible when the local Mach number is large compared to unity. (It is interesting to contrast this to a continuum calculation, which requires only that the local Mach number be greater than one, perhaps by a very small amount, for there to be no upstream influence.) In a Maxwellian gas, the probability of an individual molecule having an upstream velocity direction is given by P, where

$$P = \frac{1}{2} \text{erfc}(M \sqrt{\gamma/2}) \quad , \tag{1}$$

and M and γ denote Mach number and ratio of specific heats, respectively. For sonic flow this probability is on the order of 5%, but by the time the Mach number has become 2.0 the probability is on the order of 4×10^{-4} and, for all practical purposes, backflow can be ignored.

Hence, the imposition of the downstream boundary condition neglecting backflow into the solution region is justified very shortly after the orifice, since the flow rapidly becomes substantially supersonic. As long as this is the case, it is perfectly proper to solve for a small segment of the solution region. Once that solution is completed, then the derived velocity distribution on the downstream boundary defines the required upstream boundary condition for the next solution segment. This information is automatically written to a file which is, in turn, automatically read as input for the next segment. Segmentation can be used in conjunction with the separation of major and minor species, if desired.

2.2 Advantages of Segmentation

Although the physical justification for segmenting the solution region has been demonstrated, there remains the question

as to why one would want to "turn one problem into two or more problems." Frequently the subdivision of a physical problem into multiple subproblems reduces the total effort involved, and this is no exception. Specific advantages are enumerated below.

2.2.1 Reduced Storage

When the problem is broken up into segments, the total number of cells and molecules required in any one segment is less than required for the larger single solution. This translates directly into a decreased requirement for computer core.

2.2.2 Decreased Time to Achieve Steady Flow

The Monte Carlo technique is inherently a procedure which solves an unsteady flow problem. For cases such as the present one where the problem of interest is really a steady state flow, this is solved by letting the unsteady solution relax to a steady state. The computation time required to achieve a steady state can be regarded as "computational overhead" for the present problem, since useful steady state sampling of the solution cannot begin until steady state has been achieved.

The time required to establish a steady flow can be estimated a priori as the length of the solution region divided by the orifice flow velocity (times a safety factor). Hence, the longer the initial solution segment, the greater is the period of unsteady flow. If the entire solution region is calculated at once, then the program may well spend most of its effort in simply achieving steady state. If the solution region is segmented, however, then the first segment can reach steady state substantially faster than the whole solution region does. This is of particular significance since the solution near the

orifice is the most collision dominated, requiring a large portion of the computational effort needed in each time step. When subsequent segments are solved, they still require a relatively long time to achieve steady state (though the time is somewhat diminished since the solution region is shorter), but the computational effort per time step is substantially less.

2.2.3 Increased Time Step for Latter Segments

The time step in a Monte Carlo simulation should generally be small compared to the mean time between collisions for a molecule, since the processes of translation and collisions are treated separately in each time step. If the entire solution is solved for at once, this implies that the entire solution is constrained to the relatively small time step required by the collisional region near the orifice. If that region is solved for separately, then subsequent segments can have a substantially larger time step since the mean time between collisions is larger in subsequent segments. Hence, even though the latter regions still require a relatively large amount of simulation time to achieve steady state, this time is more easily accomplished since the allowable time step is much larger.

2.3 Segmentation Summary

These considerations strongly suggest that the first spatial segment should be made within a few diameters of the orifice, since: 1) The flow is by then already sufficiently supersonic to justify the neglect of backflowing molecules, and 2) The number of time steps required to achieve steady state is small, which is particularly important in this collision dominated region of the flow. Note that the question is completely

11

unrelated to whether or not the flow is in equilibrium (as would
be the case if an initial region were to be calculated by the
method of characteristics). It is simply a matter of making
the calculation of the flow field more efficient by separating
the relatively long relaxation time which is required by the
latter portions of the flow field from the collision dominance
which is characteristic of the initial portion. Once the first
segment is calculated, then subsequent segments benefit computa-
tionally from the ability to take substantially larger time steps
in those regions.

3. IMPROVEMENTS IN INTERNAL ENERGY MODELING

3.1 Discussion

In the previous yearly report,[1] the modeling of internal
energy of molecules and the interchange between the internal and
translational modes was discussed at length. In the past year,
significant progress was made in unifying and streamlining the
procedures for describing molecular energies, and a module was
developed which is substantially more efficient in describing
equilibrium flow. These practical improvements are fundamentally
related to the theoretical result that all of these cases can be
related to sampling from a Chi-Square distribution. The theo-
retical developments are discussed in this section, and means of
sampling from a Chi-Square distribution are discussed in the
following section.

3.2 Initial Internal Energy Levels

The classical distribution of internal energy among mole-
cules with ν degrees of freedom (Eq. (86) of Ref. 1) can be

properly simulated if each individual molecule is assigned an internal energy, E_I, given by

$$E_I = \frac{1}{2} R_0 T X \quad , \tag{2}$$

where R_0 is the universal gas constant, T is the temperature and X is a variable sampled from a Chi-Square distribution with ν degrees of freedom. (A separate sampling is made, of course, for each molecule whose internal energy is to be assigned.) This relation applies to the initialization of molecules entering the solution region through the sonic orifice. The purpose of Eq. (2) is merely to illustrate that the sampling described in the last yearly report for initial internal energy levels was essentially a sampling from a Chi-Square distribution, although it was not labeled as such.

3.3 Inelastic Bimolecular Collisions

The relations used to define the post-collision state vectors following an inelastic collision (Section 4.2 of Ref. 1) involve summing the total energy of the collision (internal energy of the two molecules plus the translational energy of their relative motion) and then redistributing it according to the number of degrees of freedom for each of the three contributing parts. The procedure involves two samplings from a distribution function, S, of the form:

$$S(\xi_1) = \frac{1}{B(\nu_1/2, \nu_2/2)} \xi^{(\nu_1/2-1)} (1-\xi_1)^{(\nu_2/2-1)} \quad , \tag{3}$$

where B denotes the beta function. Equation (3) statistically describes the partitioning of a given amount of energy between two modes, where ν_1 and ν_2 are the number of degrees of freedom

13

of the two modes, and ξ_1 is the fraction of the energy going to the mode with v_1 degrees of freedom. Equation (3) was first sampled to partition the total energy between the translational and internal modes, and then sampled again to partition the total internal energy between the two molecules.

The sampling of Eq. (3) was previously done via the acceptance-rejection method, and this was complicated by the presence of two parameters (v_1 and v_2), requiring that normalization constants either be stored in two dimensional arrays or that they be recomputed at every sampling.

As discussed in Section 4.2, the sampling of Eq. (3) can be achieved in a more basic fashion via

$$\xi_1 = \frac{X_1}{X_1 + X_2} \quad , \tag{4}$$

where X_1 is selected from a Chi-Square distribution with v_1 degrees of freedom and X_2 is selected from a Chi-Square distribution with v_2 degrees of freedom. This relation uncouples the sampling, so that it reduces the case of sampling from a two parameter distribution to that of sampling twice from a one parameter distribution. The latter approach is generally to be preferred, since optimization of the sampling routine is much easier for only one variable.

Equation (4) is a lot more signficant than merely indicating a new way to sample from the necessary distribution. As was shown in the previous section, a Chi-Square distribution describes the energy allocation that is to be expected in an equilibrium gas. Hence, Eq. (4) indicates that it is proper to first select Chi-Square values as would be done for an equilibrum gas, and then normalize the Chi-Square values selected for the various competing modes so that the available energy in a collision is precisely conserved.

This concept leads directly to an even simpler method for determining the post-collision energy distribution, namely each of the three competing modes is given a fraction of the total energy, ξ_i, given by

$$\xi_i = \frac{X_i}{X_1 + X_2 + X_3} \quad ,$$

(5)

where three Chi-Square samplings, each from a distribution with the appropriate number of degrees of freedom, replace the two samplings of Eq. (3). It is a relatively simple matter to show that Eq. (5), arrived at here intuitively, is in fact formally correct.

3.4 Equilibrium Collision Aftermath

One of the principal historic drawbacks of the direct simulation Monte Carlo method is its inefficiency (as opposed to invalidity) as collisions become more dominant and the flow approaches equilibrium. The necessity of sampling a very large number of collisions is time consuming and somewhat redundant since, once equilibrium is achieved, further collisions have no effect on the velocity distribution. This concept has been utilized in the past to cut off the sampling of collisions after the simulation of a sufficient number to guarantee equilibrium (Ref. 2), but it still required the simulation of a large number of collisions and therefore resulted in a relatively inefficient

---

[2] Bird, G. A., _Molecular Gas Dynamics_, Clarendon Press, Oxford, 1976.

15

simulation. Since the equilibrium limit is precisely the limit in which continuum fluid mechanic descriptions become valid, Monte Carlo simulations have not been extensively used in highly collisional situations.

Using the relations of this section, with some extensions, it is possible to bypass collision sampling altogether for cells in equilibrium. New velocity and internal energy elements to the state vectors can be selected directly from the distributions resulting from many collisions (i.e., equilibrium) with the constraints that total momentum and energy be precisely conserved. The result is that cells in equilibrium (i.e., those near the orifice in a mass spectrometer) can potentially become the easiest cells to simulate rather than the hardest; and the overall simulation efficiency can be substantially improved.

The procedure for sampling from the equilibrium aftermath of many collisions is as follows:

1) Evaluate the following sums over all molecules in the cell:

$$S_1 = \sum_i w_i m_i \quad , \tag{6}$$

$$S_2 = \sum_i w_i m_i u_i \quad , \tag{7}$$

$$S_3 = \sum_i w_i m_i v_i \quad , \tag{8}$$

$$S_4 = \sum_i w_i m_i w_i \quad , \tag{9}$$

$$S_5 = \sum_i w_i m_i (u_i^2 + v_i^2 + w_i^2) \quad , \tag{10}$$

and

$$S_6 = \sum_i W_i E_{Ii} \quad , \tag{11}$$

where W_i, m_i and E_{Ii} are the statistical weighting factor, the mass and the internal energy, respectively, of the ith molecule, and u_i, v_i and w_i are its velocity components.

2) Compute the center of mass velocity components, u^*, v^* and w^* via:

$$u^* = S_2/S_1 \quad , \tag{12}$$

$$v^* = S_3/S_1 \quad , \tag{13}$$

and

$$w^* = S_4/S_1 \quad . \tag{14}$$

3) The total translational energy of the relative motion between the molecules, E_{trn}, can be represented

$$E_{trn} = \frac{1}{2} \sum_i W_i m_i \left[(u_i - u^*)^2 + (v_i - v^*)^2 + (w_i - w^*)^2 \right] \, , \tag{15}$$

although it is more easily evaluated via the equivalent expression

$$E_{trn} = \frac{1}{2} \left[S_5 - \frac{S_2^2 + S_3^2 + S_4^2}{S_1} \right] \quad . \tag{16}$$

4) The total cell energy, E_{tot}, is therefore given by

$$E_{tot} = S_6 + E_{trn} \quad . \tag{17}$$

17

E_{tot}, u^*, v^* and w^* are the quantities which are to be conserved in the equilibrium sampling of new velocity and internal energy values for the cell molecules. The basic concept is to sample a Chi-Square value appropriate to each available energy mode, and then allocate the available energy in proportion to the assigned Chi-Square values. Sampling a Chi-Square value for the internal energy of each molecule is straightforward, but the translational mode requires a little care. Since it is the energy of relative motion that we are considering, and a molecule can have no relative motion with respect to itself, all but one of the molecules should have a Chi-Square value sampled for its translational degrees of freedom. (These Chi-Square values are sampled for the three translational degrees of freedom.) Velocity components of the molecules will be assigned one molecule at a time, and when this is done the center of mass velocity components of the remaining molecules are implied via conservation of u^*, v^*, and w^*. When there is only one remaining molecule this means that its velocity components are implied by the choices made for the others, and it does not have independent translational degrees of freedom. The identity of the "last" molecule is arbitrary and has no effect on the assigned velocity components.

Let X_{Ii} represent the Chi-Square value sampled for the ith molecule's internal energy mode, and X_{ti} the value sampled for its translational mode. (The last molecule is assigned $X_{ti} = 0$.) The equilibrium post-collision sampling continues as follows:

5) A weighted sum of Chi-Square values is defined via:

$$S_7 = \sum_i W_i (X_{Ii} + X_{ti}) \quad . \tag{18}$$

6) The first molecule is assigned an internal energy given by

18

$$E_{I1} = \frac{X_{I1}E_{tot}}{S_7} \quad , \qquad (19)$$

and a translational energy given by

$$E_{t1} = \frac{X_{t1}E_{tot}}{S_7} \quad . \qquad (20)$$

7) The relative speed, q_r, between the first molecule and
    the center of mass velocity of all molecules (including
    itself) which corresponds to E_{t1} is given by

$$q_r = \sqrt{2E_{t1}(S_1 - W_1 m_1)/(S_1 m_1)} \quad . \qquad (21)$$

8) The direction for the relative velocity is selected at
    random, giving the three relative velocity components
    u_{r1}, v_{r1} and w_{r1} via

$$A = 1 - 2R \quad , \qquad (22)$$

$$B = q_r \sqrt{1 - A^2} \quad , \qquad (23)$$

$$C = 2\pi R \quad , \qquad (24)$$

$$u_{r1} = q_r A \quad , \qquad (25)$$

$$v_{r1} = B\cos(C) \qquad (26)$$

and

$$w_{r1} = B\sin(C) \quad ; \qquad (27)$$

where each appearance of R denotes a distinct evalua-
tion of a random variable.

9) The updated velocity components for the first molecule
    are then given simply by:

19

$$u_1 = u^* + u_{r1} \quad , \tag{28}$$

$$v_1 = v^* + v_{r1} \tag{29}$$

and

$$w_1 = w^* + w_{r1} \quad . \tag{30}$$

10) The first molecule's contribution to u^*, v^* and w^* is then removed via the replacements:

$$(u^*)_{new} = u^* - Fu_{r1} \quad , \tag{31}$$

$$(v^*)_{new} = v^* - Fv_{r1} \tag{32}$$

and

$$(w^*)_{new} = w^* - Fw_{r1} \quad ; \tag{33}$$

where

$$F = \frac{W_1 m_1}{S_1 - W_1 m_1} \quad . \tag{34}$$

11) The first molecule's contribution to S_1 is then removed via the replacement

$$(S_1)_{new} = S_1 - W_1 m_1 \quad . \tag{35}$$

12) Steps 6 through 11 are then repeated for each molecule in the cell, except that when the last molecule is reached its velocity components are simply the center of mass velocity components, as discussed above.

Although the description of equilibrium sampling with strict conservation of total mass, momentum and energy may have seemed somewhat long, the relations are quite fast computationally,

and the increased efficiency over the sampling of many individual collisions can be substantial. The degree of increased efficiency depends, of course, on the collision rate in a particular cell.

However, some caution must be exercised in the use of the equilibrium relations. They are only justified when the number of collisions simulated in a given time step would be sufficient to guarantee equilibrium. For the translational mode this is typically on the order of three collisions per molecule, but since internal modes (usually rotation for the mass spectrometer problem) are also equilibrated, the number of collisions should be somewhat higher (typically five or so). Hence, the major disadvantage in using the equilibrium relations is the decision process required to use it only when justified. For that reason, these relations are not currently implemented in the mass spectrometer code, although they have been coded and could be inserted whenever required by a particularly collision dominated case.

4. CHI-SQUARE PROBABILITY DISTRIBUTION

4.1 Physical Basis

Fundamentally, the Chi-Square function represents the distribution of energy in an equilibrium classical system with ν degrees of freedom. It is a well known classical result that each degree of freedom for a molecule in an equilibrium gas will have, on the average, an energy of $kT/2$, where k is Boltzmann's constant and T is temperature. (For example, the translational mode, with three degrees of freedom, has an average energy of $3kT/2$ per molecule. The distribution of translational energy among the various molecules follows a Chi-Square distribution

21

with 3 degrees of freedom.) Other modes of energy (molecular rotation and vibration) have their own characteristic number of degrees of freedom, which may or may not be fully excited in the energy range of interest. If a mode is not fully excited, that simply means that it is behaving as if it had a non-integer number of degrees of freedom, within the classical approximation. The number of internal degrees of freedom is directly related to the heat capacity of the gas and, essentially, ν is selected to match the known heat capacity of a given molecule in a given energy range. The assumption of a constant number of degrees of freedom is therefore equivalent to the assumption of a constant heat capacity. A discussion of the implementation of such a model allowing for a finite rate relaxation towards equilibrium between translational and internal modes is given in Ref. 1.

4.2 Definition and Mathematical Properties[3]

The Chi-Square probability density function, $f(X;\nu)$, defines a distribution of X in a domain of zero to infinity via

$$f(X;\nu) = \frac{X^{(\nu/2 - 1)} \exp(-X/2)}{2^{(\nu/2)} \Gamma(\nu/2)} \tag{36}$$

where ν is a positive parameter of the distribution referred to as the number of degrees of freedom. The Chi-Square distribution results in a mean value of X equal to ν. Figure 1 is a plot of the Chi-Square probability density function for ν equal to 1, 2 and 3.

---

[3] Abramowitz, M., and Stegun, I.A., Handbook of Mathematical Functions, National Bureau of Standards, 1968, pp. 940, 944.
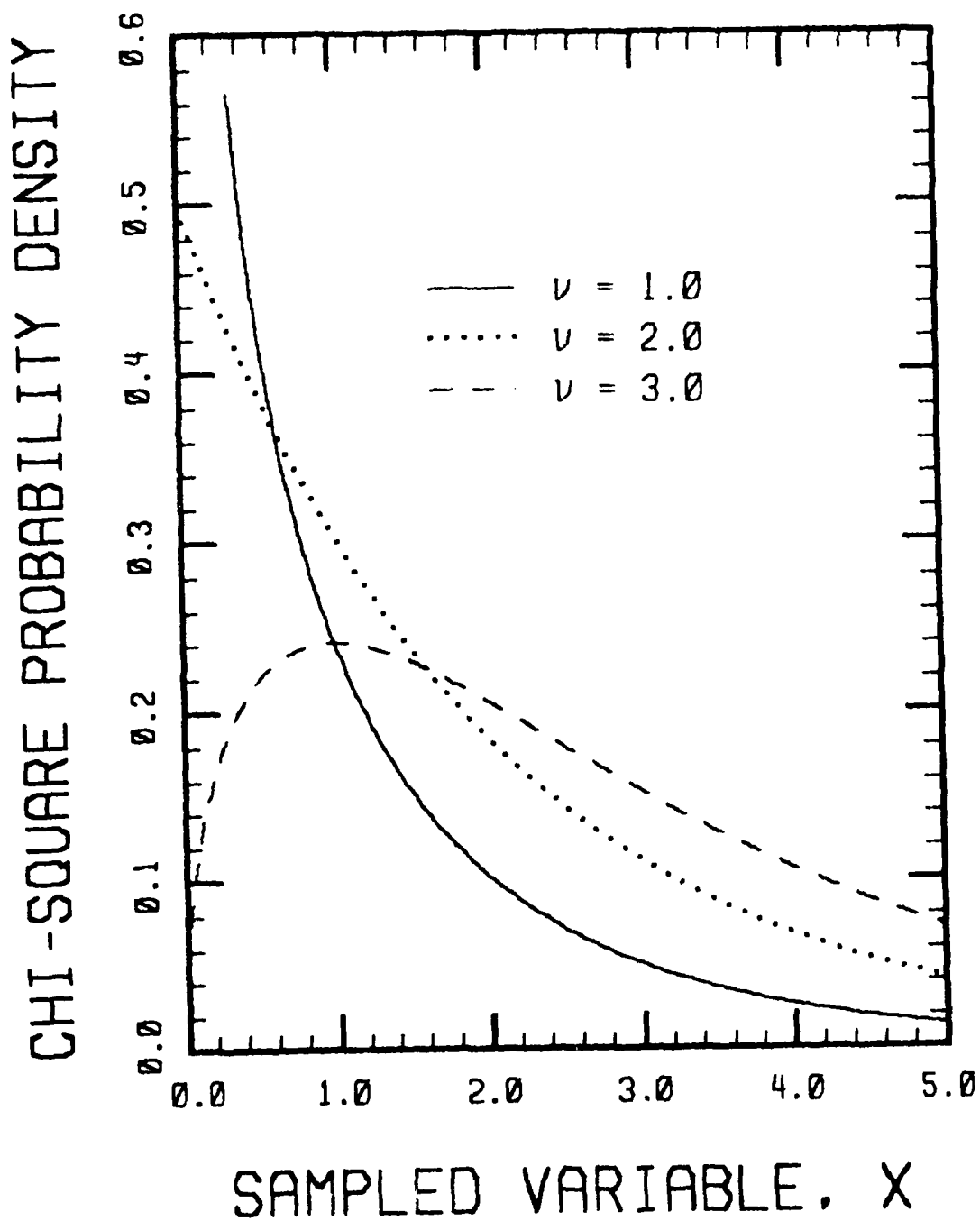
Figure 1. A Plot of the Chi-Square Probability Density
Function for ν Equal to 1, 2 and 3.

The Chi-Square distribution has a fundamental addition property such that if X_1 is selected from a Chi-Square distribution with ν_1 degrees of freedom, and X_2 is selected from a Chi-Square distribution with ν_2 degrees of freedom; then their sum will be distributed according to a Chi-Square distribution with $\nu_1 + \nu_2$ degrees of freedom. This property is of substantial theoretical and practical importance.

If the variable Z is distributed according to a normal distribution with zero mean and unit variance, then Z^2 will follow a Chi-Square distribution with one degree of freedom. It follows from the above addition property that, in general, if Z_1, Z_2, ..., Z_n are n variables selected from such a normal distribution, and X is defined as the sum of the squares of the Z_i, then the X's that result will be distributed according to a Chi-Square distribution with n degrees of freedom.

Finally, if t is distributed according to a probability desnity function $g(t;p,q)$, where

$$g(t;p,q) = \frac{t^{p-1}(1-t)^{q-1}}{B(p,q)} , \qquad (37)$$

and

$$B(p,q) = \int_0^1 t^{p-1}(1-t)^{q-1}dt = \frac{\Gamma(p)\Gamma(q)}{\Gamma(p+q)} , \qquad (38)$$

(B is the Beta function) then t can be sampled via

$$t = \frac{X_1}{X_1 + X_2} , \qquad (39)$$

where X_1 is selected from a Chi-Square distribution with ν_1 degrees of freedom, and X_2 is selected from a Chi-Square distribution with ν_2 degrees of freedom, with

$$\nu_1 = 2p \quad , \tag{40}$$

and

$$\nu_2 = 2q \quad . \tag{41}$$

The significance of Eq. (39) is that it reduces the sampling from
a two parameter distribution (Eq. (37)) to two samplings from a
one parameter distribution. The distribution represented by
Eq. (37) arises in cases where a constrained amount of total
energy is distributed among various modes, and its relation to
the Chi-Square distribution apparently has not been appreciated
by developers of techniques for Monte Carlo fluid mechanics.

4.3 Sampling From a Chi-Square Distribution

The need for sampling from a Chi-Square distribution comes
up when sampling initial values of internal energies, when
calculating inelastic collisions via the statistical collision
model[4] or when calculating the equilibrium aftermath of many
collisions in a cell. Since these operations must be performed
repeatedly in the heart of a Monte Carlo simulation, it is import-
ant that the sampling be done efficiently and accurately.

For clarity, the result of each sampling method discussed
below will be denoted by a different letter subscript to X.
All sampling procedures make use of a random number generator
which returns a number, R, selected from a probability density
which is uniform on the interval between zero and one. Each
occurrence of R indicates a distinct sampling from the random
number generator.

---

[4] Borgnakke, Claus, and Larsen, Paul S., "Statistical Collision
Model for Monte Carlo Simulation of Polyatomic Gas Mixture,"
Journal of Computational Physics, Vol. 18, 1975, pp. 405-420.

4.3.1 Analytic Sampling for Integer ν

Direct sampling of Eq. (36) can be performed for integer ν, as shown below.

4.3.1.1 $\nu = 0$

As ν (an intrinsically nonnegative quantity) approaches zero, the distribution function approaches a delta function, and a proper sampling is achieved by simply selecting

$$X_a = 0 \quad . \tag{42}$$

4.3.1.2 $\nu = 1$

For sampling with $\nu = 1$ (as well as for several other cases) it is convenient to introduce the transformation $Z^2 = X$. Z is then distributed according to the probability density function $p(Z)$ given by

$$p(Z) = \frac{Z^{(\nu-1)} \exp(-Z^2/2)}{2^{(\nu/2 - 1)} \Gamma(\nu/2)} \quad . \tag{43}$$

For $\nu = 1$, this distribution is simply a normal distribution adjusted to allow for positive only argument. Sampling from this distribution is described in Ref. 3. When the result is cast back in terms of X, the result is

$$A = 2\pi R \tag{44}$$

and

$$X_b = -2\log(R)\sin^2(A) \quad . \tag{45}$$

4.3.1.3 $\nu = 2$

When $\nu = 2$, the integral of Eq. (36) can be analytically inverted, leading to the direct sampling

$$X_c = -2\log(R) \quad . \tag{46}$$

4.3.1.4 ν Equal to an Even Integer

The extreme simplicity of the above sampling for $\nu = 2$, together with the addition property of the Chi-Square distribution, means that sampling for ν equal to an even integer is quite direct. Let $J = \nu/2$, then a proper Chi-Square sampling is given by

$$X_d = -2\log(R_1 R_2 \ldots R_j) \quad , \tag{47}$$

where R_1 through R_j denote j samplings from the random number generator. The fact that the log need only be taken once in Eq. (47) means that the evaluation of X_d is quite efficient, even for moderately large ν.

4.3.1.5 ν Equal to an Odd Integer

For ν equal to an odd integer, the addition property of the Chi-Square distribution allows the simple combination of the results for ν equal to one and ν equal to an even integer, i.e.,

$$X_e = X_b + X_d \quad , \tag{48}$$

where X_b is given in Eq. (45) and X_d is given in Eq. (47) with $J = (\nu-1)/2$.

4.3.2 Generalized Acceptance-Rejection Sampling

For non-integer ν, it is necessary to use a generalized form of acceptance-rejection sampling. Before the application to Chi-Square sampling is presented, the acceptance-rejection technique and its generalization will be briefly discussed.

4.3.2.1 Standard Acceptance-Rejection Sampling

The usual acceptance-rejection technique for sampling from a general distribution function, $p(x)$, proceeds as follows:

1) The domain of x is approximated, if necessary, by a finite sub-domain.

2) The maximum value of $p(x)$, p^*, is calculated.

3) A variable ξ is selected from the domain of x via

$$\xi = x_{min} + R(x_{max} - x_{min}) \quad .$$

4) $p(\xi)/p^*$ is calculated, and another random variable, R is generated. x is set equal to ξ if R is less than $p(\xi)/p^*$.

5) Steps 3 and 4 are repeated until a value of x is determined.

Note that the probability of acceptance of the random variable in step 4 is proportional to the distribution function being sampled, so the resulting x values will follow the desired distribution function.

Although the generality of this approach makes it very powerful, it does suffer from the following drawbacks:

- If the distribution function differs significantly from its maximum value within a substantial portion of the sampled domain, then the rejection rate may be high. This obviously leads to a slow sampling procedure.

- If the finite sub-domain is reduced to increase the acceptance rate, then the sampling deviates from the true distribution function.

- The procedure is incapable of sampling from an unbounded distribution function.

4.3.2.2 Generalization of the Acceptance-Rejection Technique

The following procedure comprises a generalization of the *acceptance-rejection technique*:

1) A second distribution function, $q(x)$, which can be sampled analytically is chosen. Conditions on $q(x)$ will be discussed below.

2) The maximum value of $p(x)/q(x)$, $(p/q)^*$, is calculated.

3) A variable, ξ, is sampled from q.

4) $Q = \left[p(\xi)/q(\xi)\right]/(p/q)^*$ is calculated, and another random variable, R, is generated. x is set equal to ξ if R is less than Q.

5) Steps 3 and 4 are repeated until a value of x is determined.

It should be noted that the probability density for a given value of x is proportional to the product of the initial selection probability times the acceptance probability. Since the former probability is proportional to $q(x)$, and the latter is proportional to $p(x)/q(x)$, the distribution of accepted values does indeed follow the distribution function $p(x)$.

The usual *acceptance-rejection technique* is simply the case where $q(x)$ is constant, but it is evident that this is not always the best (or even a possible) choice. All of the

29

objections to the standard acceptance-rejection technique can
be removed or ameliorated by a suitable choice for q(x). In
particular:

- There is no need to approximate the domain of x with
  a finite sub-domain. It is merely necessary that the
  domain for q include the domain for p. The domain
  for q can be larger than that for p, since whenever a
  value is selected from outside the domain for p it
  will always be rejected in step 4 above.

- If q is selected to be close to p, at least in the
  region of highest probability, then the acceptance
  rate of trial values will be large.

- Unbounded distribution functions can be sampled if
  q is chosen to have the same type of singularity as
  p, since the only requirement is that the ratio (p/q)
  remain bounded.

For any given situation, the choice of the function q is
a bit of an art, guided by the concerns highlighted above: q
must have a domain which includes the domain of p; p/q must
remain bounded; and (p/q) should achieve its maximum in the
vicinity of the maximum of p.

4.3.3 Exact Acceptance-Rejection Sampling for a Chi-Square Distribution with Large ν

The acceptance-rejection technique described above can be
used to achieve an exact sampling from a Chi-Square distribution
for large ν. (Actually, the approach is perfectly valid for
all $\nu > 1$, but the method to be described in Section 4.3.5 is
to be preferred for $\nu < 45$, or so.) The procedure utilizes the
transformed Chi-Square distribution, p(Z), given by Eq. (43) as

the distribution to be sampled. A normal distribution is used as the initial distribution which can be sampled analytically. The normal distribution is chosen to have a unit variance and a mean which corresponds to the location of the maximum of $p(Z)$. This maximum occurs at Z^* given by

$$Z^* = \sqrt{\nu - 1} \quad . \tag{49}$$

The functional form of the normal distribution, $q(Z)$, is

$$q(Z) = \exp\left[-(Z - Z^*)^2\right]/\sqrt{2\pi} \quad , \tag{50}$$

which not only has a maximum at the same location as Eq. (43), but has the same exponential factor as Z approaches infinity and a domain which includes that of Eq. (43). The sampling of a Chi-Square value proceeds as follows:

1) $Z^* = \sqrt{\nu - 1}$ is calculated.

2) A sample from the distribution given by Eq. (51) is taken via:

$$A = 2\pi R \tag{51}$$

$$B = -\log(R) \tag{52}$$

$$Z = Z^* + \sqrt{2B}\sin(A) \tag{53}$$

3) The acceptance probability, Q, is computed as

$$Q = (Z/Z^*)^{(\nu - 1)}\exp\left[-Z^*(Z - Z^*)\right] \quad . \tag{54}$$

(Q is taken to be zero for negative Z.)

4) Another random variable is generated, and Z is kept if $Q > R$. If Z is rejected, then steps 2-4 are repeated until a Z value is accepted.

31

5) When a Z value is accepted, then the corresponding Chi-Square value is given by

$$X_e = Z^2 . \tag{55}$$

This procedure is illustrated in Fig. 2 which shows $p(Z)$, $q(Z)$ and $Q(Z)$ for $\nu = 50$. Note that the acceptance probability is near unity in the vicinity of the maxima of the two distribution functions, so a large fraction of the selected samples of $q(Z)$ will be accepted as samples of $p(Z)$.

4.3.4 Exact Acceptance-Rejection Sampling for a Chi-Square Distribution with $(0 < \nu < 2)$

For this domain of ν it is convenient to introduce another transformation to Eq. (36). If W is defined by

$$W = \exp(-X/2) , \tag{56}$$

then the probability density function for W is given by $h(W)$, where

$$h(W) = \frac{\left[-\log(W)\right]^{(\nu/2 - 1)}}{\Gamma(\nu/2)} . \tag{57}$$

The domain for W is finite (between 0 and 1), but $h(W)$ becomes infinite as W approaches unity. The generalized acceptance-rejection technique can still be used, however, since the function $q(W)$ given by

$$q(W) = (\nu/2)(1 - W)^{(\nu/2 - 1)} \tag{58}$$

has the same type of singularity and can be analytically sampled. The Chi-Square sampling for $(0 < \nu < 2)$ proceeds as follows:
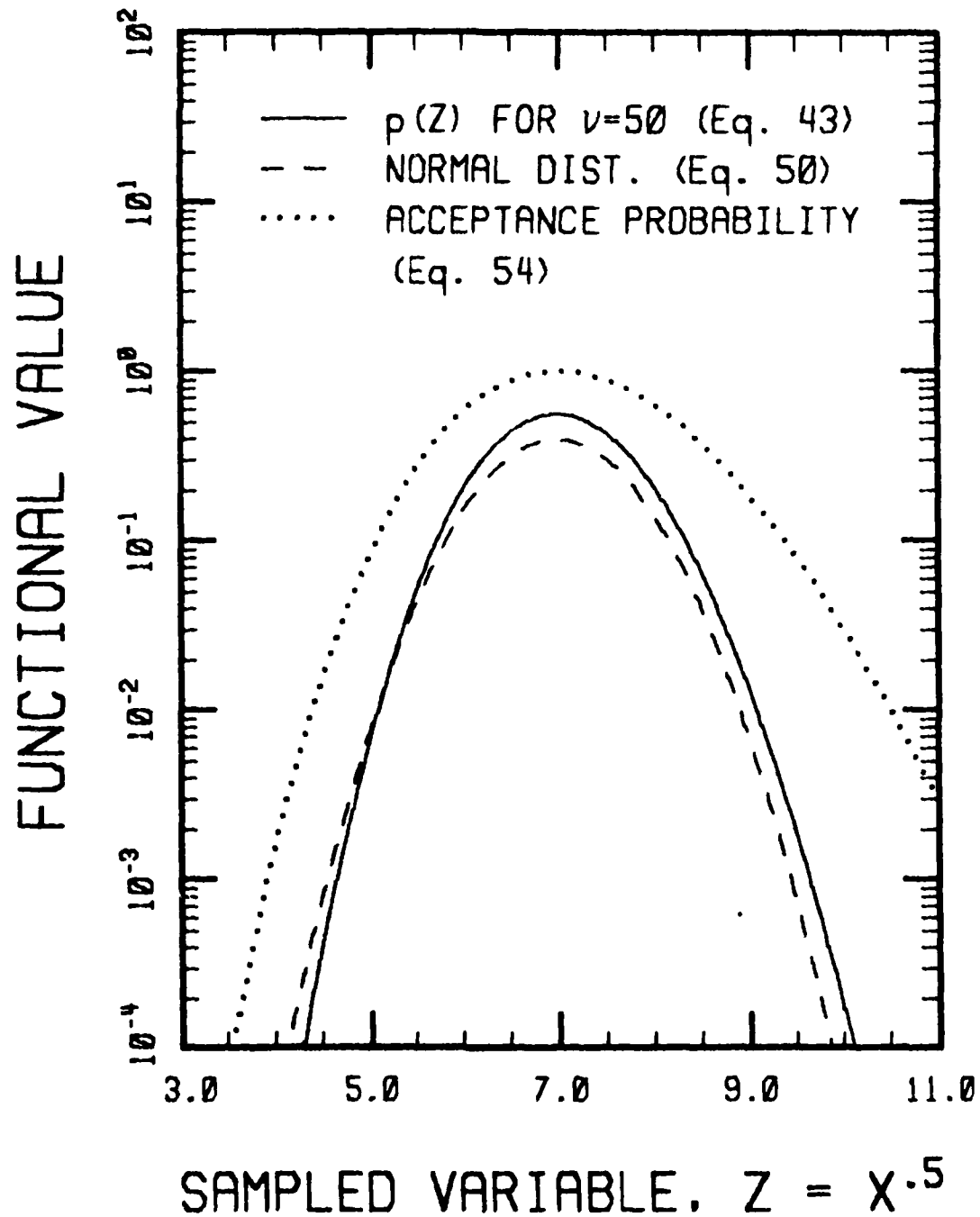
Figure 2. A Representation of the Transformed Chi-Square Distribution, $p(Z)$, for $\nu = 50$ (solid line). $p(Z)$ is sampled by first selecting a variable from the shifted normal distribution (dashed line) and keeping it with a probability given by $Q(Z)$ (dotted line).

33

1) A sample from q(W) is generated via

$$W = 1 - R^{(2/\nu)} \quad . \tag{59}$$

2) The acceptance probability, Q, is computed from

$$Q = \left[(W - 1)/\log(W)\right]^{(1 - \nu/2)} \quad . \tag{60}$$

3) Another random variable, R, is generated, and W is kept if Q > R; otherwise steps 2 and 3 are repeated until a value for W is accepted.

4) When a value for W is accepted, the corresponding Chi-Square value is given by

$$X_f = -2\log(W) \quad . \tag{61}$$

This procedure is illustrated in Fig. 3, which shows the two distribution functions, h(W) and q(W), and the acceptance probability, Q(W), for $\nu = 1$. It can be seen that q(W) provides an excellent choice for the initial selection of W, since the acceptance probability remains high throughout the important domain of W. This point will be discussed in more detail in Section 4.3.6.

4.3.5 Exact Chi-Square Sampling for General ν

Using the fundamental addition property of Chi-Square distributions, it is possible to combine the procedure described in Section 4.3.1.4 for ν equal to an even integer with the procedure described in Section 4.3.4 for $(0 < \nu < 2)$ to achieve an exact general sampling technique for arbitrary ν. This is given simply by
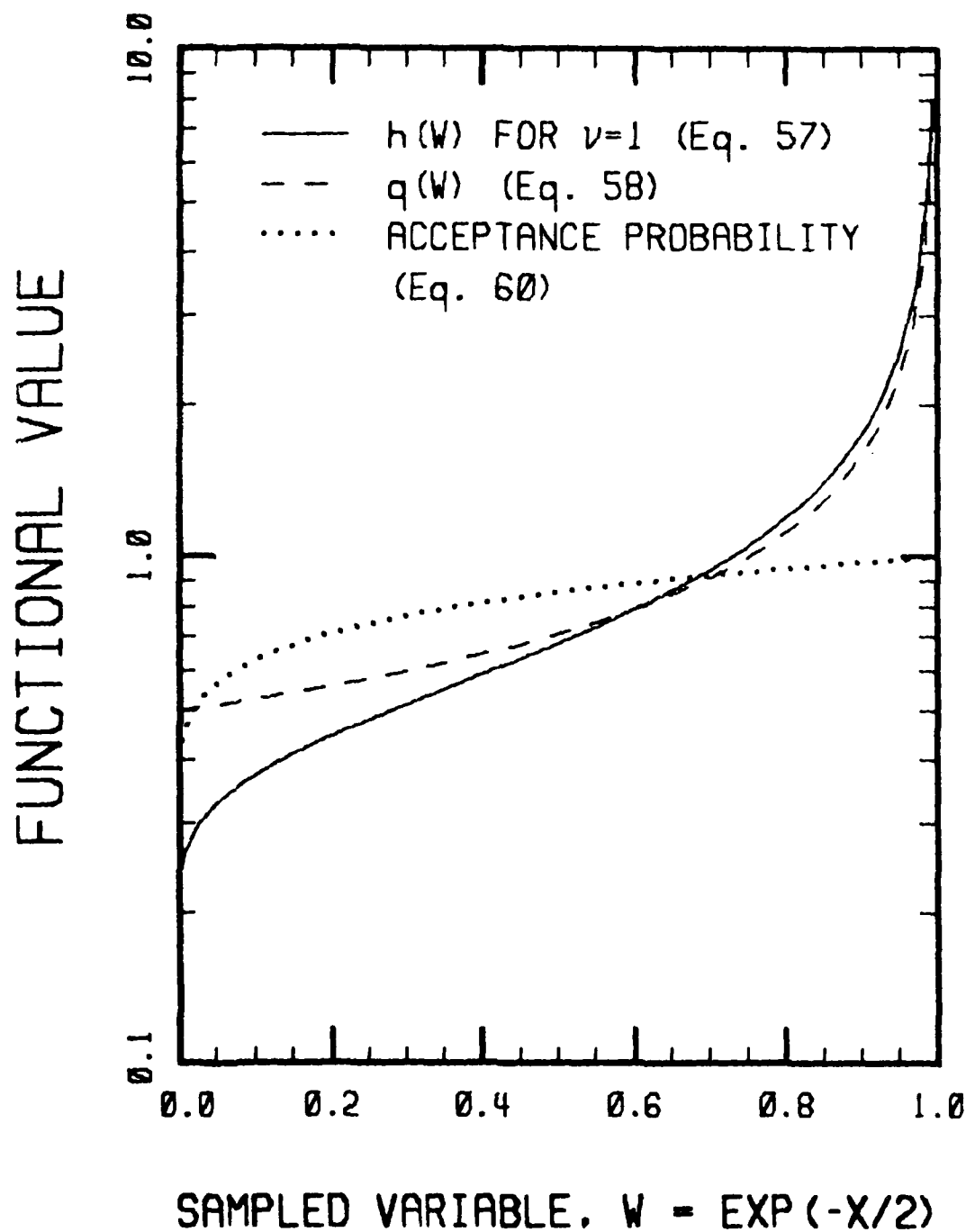
$$X_g = X_d + X_f \quad , \tag{62}$$

Figure 3. A Representation of the Transformed Chi-Square Distribution, h(W), for $\nu = 1$ (solid line). h(W) is sampled by analytically selecting a variable from q(W) (dashed line) and keeping it with a probability given by Q(W) dotted line).

where X_d is calculated from Eq. (47) with J equal to the integer portion of $\nu/2$, and X_f is calculated as in the preceding section with ν being replaced by $\nu - 2J$.

It is to be noted that both the approach given in this section (Eq. (63)) and that given in Section 4.3.3 (Eq. (55)) are exact and applicable for $\nu > 1$. In general, the approach of this section is considerably faster, although as ν gets large the approach of Section 4.3.3 becomes more attractive. There are two potential difficulties with Eq. (62) as ν becomes very large. Firstly, the product required in Eq. (47) gets more and more cumbersome to compute as ν increases, and, secondly, the larger the number of factors in this product the greater is the chance that it will yield a number so small as to produce a floating point underflow on a computer. (Since Monte Carlo codes must be highly reliable, any such problem should be made essentially impossible.) It turns out that the second problem is more restrictive (at least for 32 bit computers), dictating that the Eq. (55) should be used for ν greater than 45, or so. This keeps the probability of an underflow below 10^{-10} on any given sampling.

4.3.6 Approximate Chi-Square Sampling for $(0 < \nu < 2)$

The procedure described in the preceding section is quite efficient, but it is nonetheless useful to consider approximate methods for sampling from Chi-Square distributions. While it would be scarcely possible to improve on sampling for even integer ν discussed in Section 4.3.1.4, it is reasonable to investigate approximations for the $(0 < \nu < 2)$ portion discussed in Section 4.3.4. A likely place to look for useful approximations in this procedure is in the calculation of Q (Eq. (60)),

36

which must be performed for every W selected in Eq. (59). (Note that the calculation of Q involves more computational effort than the calculation of W.)

The overall probability that the value chosen in Eq. (59) will be kept as a sample of Eq. (57) is given by P, where

$$P = \int_0^1 q(W)Q(W)dW = \Gamma(1 + \nu/2) \quad . \tag{63}$$

Hence, as ν approaches 0 or 2, all initially selected values of W are kept as valid samples of Eq. (57) and the computation of Q serves no useful purpose. In the worst case ($\nu = 0.92$) the overall acceptance probability is 89%, and only 11% of the initially selected variables are rejected. The approximate Chi-Square sampling involves approximating $Q(W)$ by an easily calculable function which differs little from Eq. (60). The current approximation is $Q_a(W)$, given by

$$Q_a(W) = 1 - (1 - \nu/2)(1 - W)\left[.5 + \alpha(\nu)(1 - W)^2\right] \quad , \tag{64}$$

where

$$\alpha(\nu) = .2511\nu + .2073 \quad . \tag{65}$$

Q_a was selected to match the value and slope of Q at $W = 1$, which is the region of highest probability density. The coefficient $\alpha(\nu)$ is a linear fit to values chosen to be optimal in the least squares sense. A comparison of Q and Q_a for $\nu = 1.0$ is shown in Fig. 4, which demonstrates the substantial accuracy of the approximation.

It is fundamentally more important, of course, to compare the correct Chi-Square distribution with the distribution which is effectively being sampled in the approximate technique. If
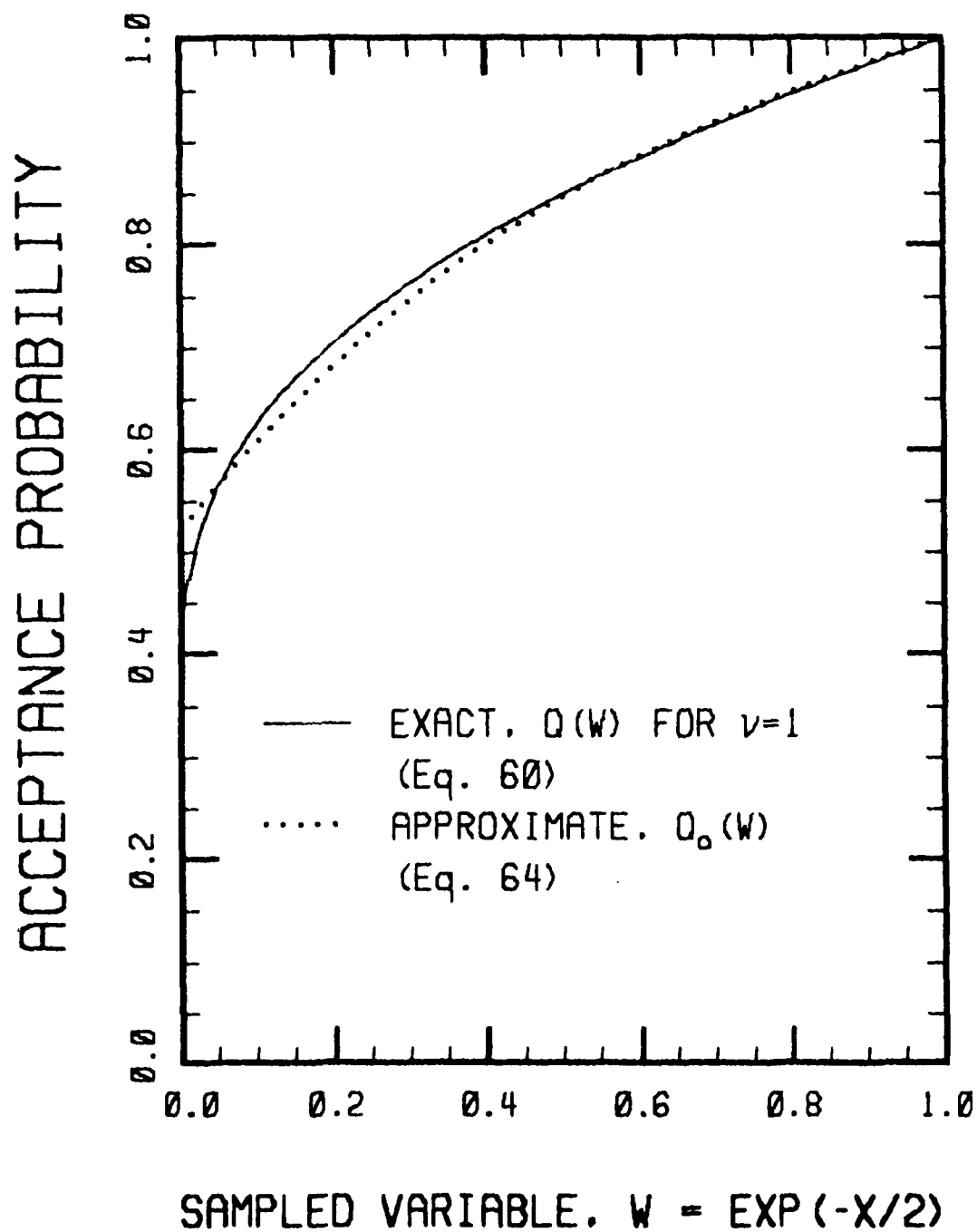
37

Figure 4. A Comparison of the Exact and Approximate
Acceptance Probabilities for $\nu = 1$.

$h_a(W)$ is the approximation analog of $h(W)$, then $h_a(W)$ is proportional to the product $q(W)Q(W)$, i.e.,

$$h_a(W) = A(1 - W)^{(\nu/2 - 1)} Q_a(W) \quad , \tag{66}$$

where the normalization factor, A, is determined by requiring that $h_a(W)$ give unity when integrated between zero and one. This results in

$$\frac{1}{A} = \frac{\nu^2 + 2\nu + 8}{2\nu^2 + 4\nu} + \frac{2\alpha(\nu)}{\nu + 6} \quad . \tag{67}$$

Once $h_a(W)$ is defined, the corresponding distribution function for X, $f_a(X;\nu)$ is obtained by multiplying $h_a(W)$ by the magnitude of dW/dX ($=W/2$), and substituting $W = \exp(-X/2)$. The comparison between $f(X;1.0)$ and $f_a(X;1.0)$ is given in Fig. 5, and the agreement is excellent. The use of the approximate technique is approximately 40% faster than the exact acceptance-rejection technique, and the difference in the distributions being sampled will probably always be negligible. Although the ability to sample from an exact Chi-Square distribution will be kept as an option, it is felt that the approximate technique offers a substantial time savings for an inconsequential loss of accuracy.

5.   INCLUSION OF ELECTRIC FIELD EFFECTS

5.1 Acceleration of Charged Species

An essential element of the computational model is the accelerating effects of electric fields on charged species. The program was generalized this year so that axial position and velocity elements of a molecular state vector are updated to include the effect of electric fields in the portion of the
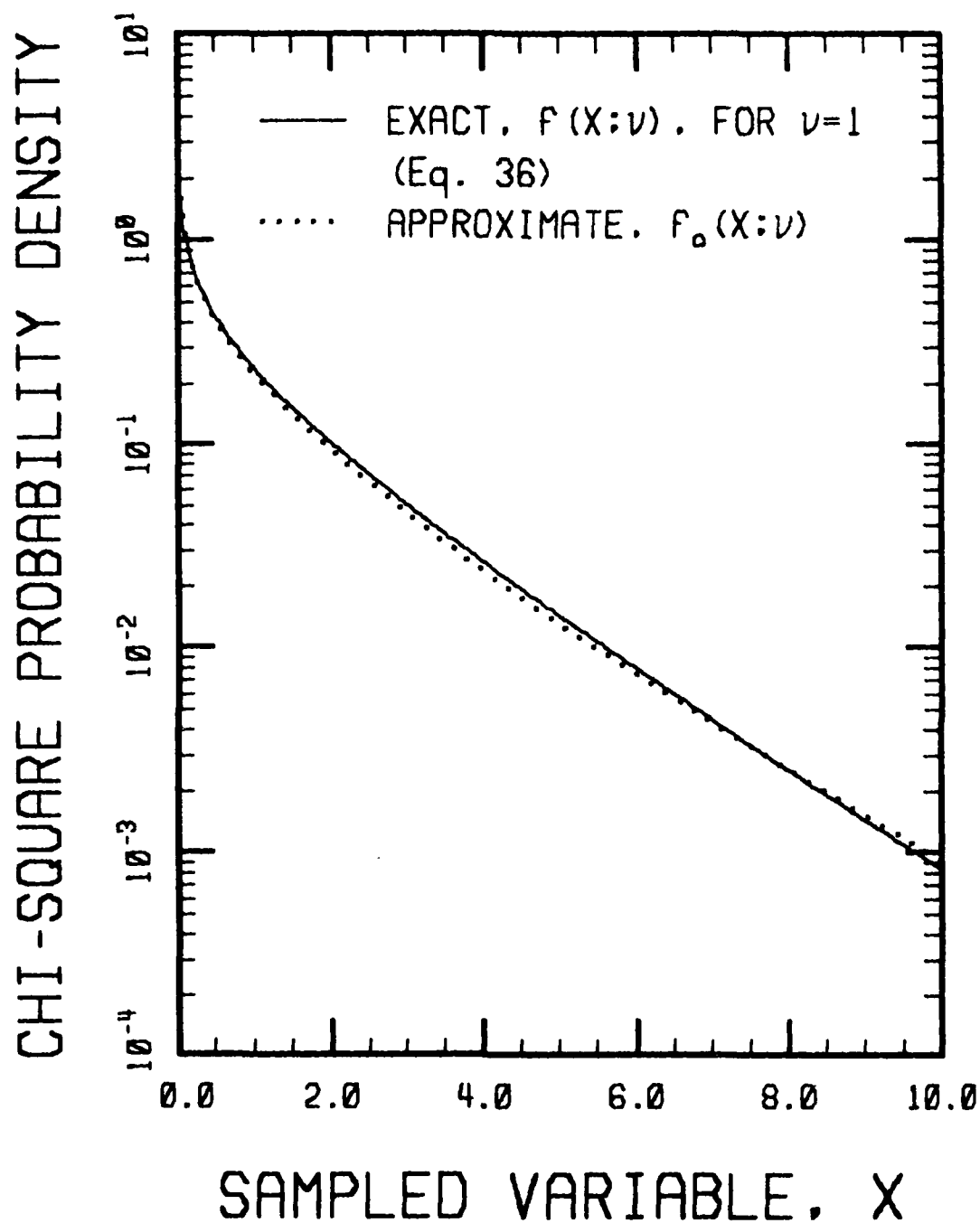
39

Figure 5. A Comparison of the Exact Chi-Square Distribution, $f(X;\nu)$ with the Approximate Distribution, $f_a(X;\nu)$ which is Effectively Being Sampled by the Approximate Technique Presented in Section 4.3.6. ν was taken to be unity for the comparison.

program that advances the molecules along their trajectories.
(The term molecule is used here in a general sense, and is meant
to apply to cluster ions as well.) If a molecule has an initial
axial position and velocity given by z_0 and v_{z0}, then after a
time t, its axial position and velocity will be given by z_1 and
v_{z1}, where

$$z_1 = z_0 + t(v_{z0} + \frac{qEt}{2M}) \tag{68}$$

and

$$v_{z1} = v_{z0} + \frac{qEt}{M} \quad . \tag{69}$$

In these relations, which replace Eqs. (58) and (61) of Ref.
1, q is the molecular charge, M is the molecular mass and E is
the local electric field strength. The electric field strength
is calculated from

$$E = -\nabla\phi \quad , \tag{70}$$

where ϕ denotes the electric potential. The electric field is
assumed to be one dimensional in the axial direction, and is
calculated from input grid voltages and positions. (The assump-
tion of one dimensionality is consistent with the geometry of
the mass spectrometer and the primary interest of flow along
the axis of symmetry.) Note that for q = 0, the above relations
reduce to Eq. (58) and Eq. (61) of Ref. 1 as applied to uncharged
species.

5.2 Neglect of Space Charge Contribution to E

The calculation of E from the input grid conditions, neglect-
ing the contribution from the ions in the flow, is a considerable
simplification which results in an uncoupling of the electric and

41

flow field problems. The validity of this approximation for the case of interest can be demonstrated via a simplified example. Consider two grids of potentials ϕ_1 and ϕ_2, with the former being located at $z = 0$ and the latter being located at $z = s$. If there is a uniform space charge density, ρ, between the plates, then the potential between the plates is determined as the solution to Poisson's equation:

$$\nabla^2 \phi = \frac{d^2 \phi}{dz^2} = -\frac{\rho}{\varepsilon_0} \quad . \tag{71}$$

which is

$$\phi = \phi_1 + (\phi_2 - \phi_1)\frac{z}{s} + \frac{\rho}{\varepsilon_0} z(s - z) \quad . \tag{72}$$

(In these relations, ε_0 is the permittivity of free space, equal to 8.855×10^{-12} farad/m.) The corresponding electric field strength is then computed as

$$E = -\frac{d\phi}{dz} = \frac{\phi_1 - \phi_2}{s} 1 + H(\frac{2z}{s} - 1) \quad , \tag{73}$$

where the dimensionless parameter, H, is defined by

$$H = \frac{\rho s^2}{2\varepsilon_0 (\phi_1 - \phi_2)} \quad . \tag{74}$$

The purpose of this exercise has been to determine the dimensionless parameter which determines when space charge has a significant effect on the electric field distribution. That parameter is H, and it can be seen from Eq. (72) that the electric field distribution is unaffected by space charge as long as H is small compared to unity.

A conservative estimate of H for the problem of interest is obtained by taking a typical potential difference of 10 volts

existing between plates separated by a distance on the order of 0.01 meter. ρ can be grossly overestimated by taking the ambient ion density ($\sim 10^9$ m^{-3}) times the electronic charge (1.6×10^{-19} coulomb), neglecting the mitigating effects of charge balance and the density reduction in a vacuum expansion. Even with this substantial overestimate, H is on the order of 10^{-4}, and the perturbation of the electric field due to space charge is quite negligible.

6. SUMMARY OF CODE STATUS

With all the technical detail presented in this and the previous yearly report, it is useful to give an overview of the code current status. The program is (temporarily, at least) called the EXPANDO code, and it currently has 36 subroutines comprising over 4100 lines of FORTRAN. It is written in a highly modular fashion, so that new capabilities can be included without major modifications of the code. There has been a substantial effort to make the code efficient in its utilization of computational resources. As a result of this, all runs to date have been performed satisfactorily on a micro-computer. The performance on a larger computer is naturally expected to be even better.

The code implements and expands the direct simulation Monte Carlo method for transitional gas dynamics, as applied to the flowfield beyond the orifice in a mass spectrometer. By directly simulating the molecular processes of translations, collisions and chemical reactions it retains validity even though the formalism of continuum fluid mechanics breaks down in this case. Some of the specific features of the EXPANDO code are:

- It can treat an arbitrary number of species and an arbitrary number of chemical reactions between them.

- The species are allowed to have internal energy, and the code describes the nonequilibrium process by which the internal modes go out of equilibrium with the translational mode.

- Species are allowed to interact with a velocity dependent gas kinetic cross section. This is a particularly important feature for the mass spectrometer problem since the static temperature of the free jet expansion changes so radically as the flow expands from the orifice.

- It can treat the flowfield between the orifice and the skimmer in one run, or it can break up the flowfield into multiple segments and solve for them separately.

- It can solve for the gas dynamic flowfield of the major neutral species separately and then go back and calculate the minor species solution as a perturbation.

- Ionic species are allowed, and the accelerating effects of electric fields produced by charged grids can be simulated.

- The code performs self checks, to make sure, for instance, that the collision rate is being simulated properly.

Only two major capabilities must be added to the program. First, the reflection of jet molecules off the skimmer must be simulated to make sure that there is no substantial skimmer

44

interference in the molecular beam. Since the skimmer will be cryogenically cooled, the code will allow for a fraction of the molecules impacting the skimmer wall to stick. Those that do not stick will specularly reflect off the skimmer. The second new feature is the ability to describe a background gas within the mass spectrometer which may intrude into the jet and degrade the beam quality. (This background gas is also a result of a sticking coefficient being less than unity.)

It should be stressed that merely writing a computer program does not comprise the totality of the present effort. There is also further work to be done in the characterization of the cross sections for the critical agglomeration and fragmentation processes that are to be simulated. The computer program can only predict the macroscopic implications of these cross sections; the generation of the proper input requires sound scientific judgement. This will be a major task for the final year on this contract.

7. DATA COMPARISON FOR SPECIES SEPARATION

To serve as a test f the basic physics and numerics embodied in the code, it was deemed desirable to make a calculational comparison with published data as a verification. Naturally, this comparison can only involve features of the code which have already been instituted. The data that were chosen for comparison involve the separation of CO_2 and H_2 in a free jet expansion, as published in Ref. 5. The case selected involves a Reynold's number which is in the relevant range for the mass spectrometer flow problem.

---

[5]McCay, T. D., and Price, L. L., "Diffusive separation of binary mixtures of CO_2-H_2 in a sonic-orifice expansion," Physics of Fluids, 26(8), August 1983, pp. 2115-2119.

45

7.1 Problem Definition

The case of interest involves producing a free jet expansion from a reservoir which has a CO_2 mole fraction of 94.9%, with the remaining 5.1% being H_2. The stagnation temperature was 286 K, and the stagnation pressure is estimated to be 1.48×10^3 dyne/cm^2. (It was necessary to estimate the stagnation pressure since this quantity was not given by the experimenters. The Reynold's number based on the stagnation speed of sound and the orifice diameter was supplied, but the viscosity on which the Reynold's number was based was not given either. Since the viscosities are well known for these gases, the error induced here is probably negligible.) The gas was expanded through a sonic orifice of 0.32 cm diameter, and the species concentrations were measured via electron beam fluorescence. The data were presented as the ratio of CO_2 to H_2 concentrations on the jet axis as a function of distance downstream from the orifice.

7.2 Computational Considerations

Effective cross sections for CO_2 and H_2, together with their energy dependence, are given by Bird.[6] In calculating the jet expansion, CO_2 was taken to have 2.0 internal degrees of freedom, since its vibrational energy rapidly freezes. The orifice conditions were based on equilibrium, however, with CO_2 having 3.58 internal degrees of freedom. (H_2 was taken to have 2.0 internal degrees of freedom throughout the calculation.) The discharge coefficient was calculated using the relations for N_2 as being

---

[6]Bird, G. A., "Monte-Carlo Simulation in an Engineering Context," Proceedings of the 12th International Symposium on Rarefied Gas Dynamics, Vol. 74, Progress in Astronautics and Aeronautics, AIAA, New York, 1981.

0.87. (Although this is certainly not precise, it is also an acceptable approximation for the present purposes.) The grid structure described in Ref. 1 was employed, with the orifice radius being divided into six cells, and three additional cells added beyond the outside of the orifice for a total of nine cells in the radial direction. Subsequent downstream cells were enlarged to keep pace with the expanding jet, until a total of twenty axial stations (180 cells altogether) were utilized.

Since 95% of the flow was CO_2, it was reasonable to perform this calculation using the ability to separately compute major and minor species. Accordingly, the CO_2 distribution was first calculated assuming no H_2 to be present. After the CO_2 jet was defined, the calculation for H_2 diffusing through the CO_2 was performed, allowing the H_2 to suffer collisions with itself as well as CO_2.

The calculation of the H_2 flow involved some special problems which were fairly specific to its light molecular weight. Since the H_2 is over 20 times lighter than CO_2, its thermal velocity is between 4 and 5 times as large as that for CO_2. This has two implications of importance for the calculation. First, spatial segmentation of this solution was not feasible. This was because the effective Mach number of the H_2 (considered by itself) remained quite small. This can be seen by considering an equilibrium mixture flowing at high speed. If the flow is in equilibrium, then the mean velocity and temperature of each component of the mixture will be the same. For a lighter gas, however, a given temperature translates into a larger thermal velocity, and the Mach number of the lighter component considered alone is less than that for the mixture. The same statement is basically true for the nonequilibrium situation of interest here. Although there were velocity and temperature

slips between the two components of the mixture, the effective Mach number of the H_2 remained small enough so that it was not reasonable to truncate the solution region and neglect backflow of H_2 molecules. Therefore, the solution was carried out in one segment to an axial distance of approximately ten orifice diameters (the extent of the data).

The second problem of relevance was the time step involved. The time step should be small compared to the mean time between collisions for a given molecule, and a molecule of H_2, with its much larger thermal velocity, suffers collisions at a much faster rate than a molecule of CO_2. Hence, for the minor species run, the time step was reduced by a factor of $\sqrt{22}$. It should be noted that the ability to separate major and minor species enabled the major species to be treated with a much larger time step than the minor species. If one solution were carried out combining major and minor species, then the entire solution would have to be limited by the time step required by the H_2.

The ability to compute minor species with a different time step than that used for major species does have relevance to the mass spectrometer flow problem. In that problem, the minor species of interest will include charged species which are accelerated by electric fields relative to the rest of the flow. Such molecules will have an elevated collision frequency and will therefore require a smaller computational time step in order to assure that the time step is small compared to the mean time between collisions. With the ability to separate major and minor species, the entire solution need not be computed under this restriction; it is only necessary to apply it when determining the minor species solution.

7.3 Results

The comparison of the calculational results with the published data is shown in Fig. 6. The agreement is excellent. This is felt to be a strong confirmation of the code's ability to calculate a basic free jet flow field.
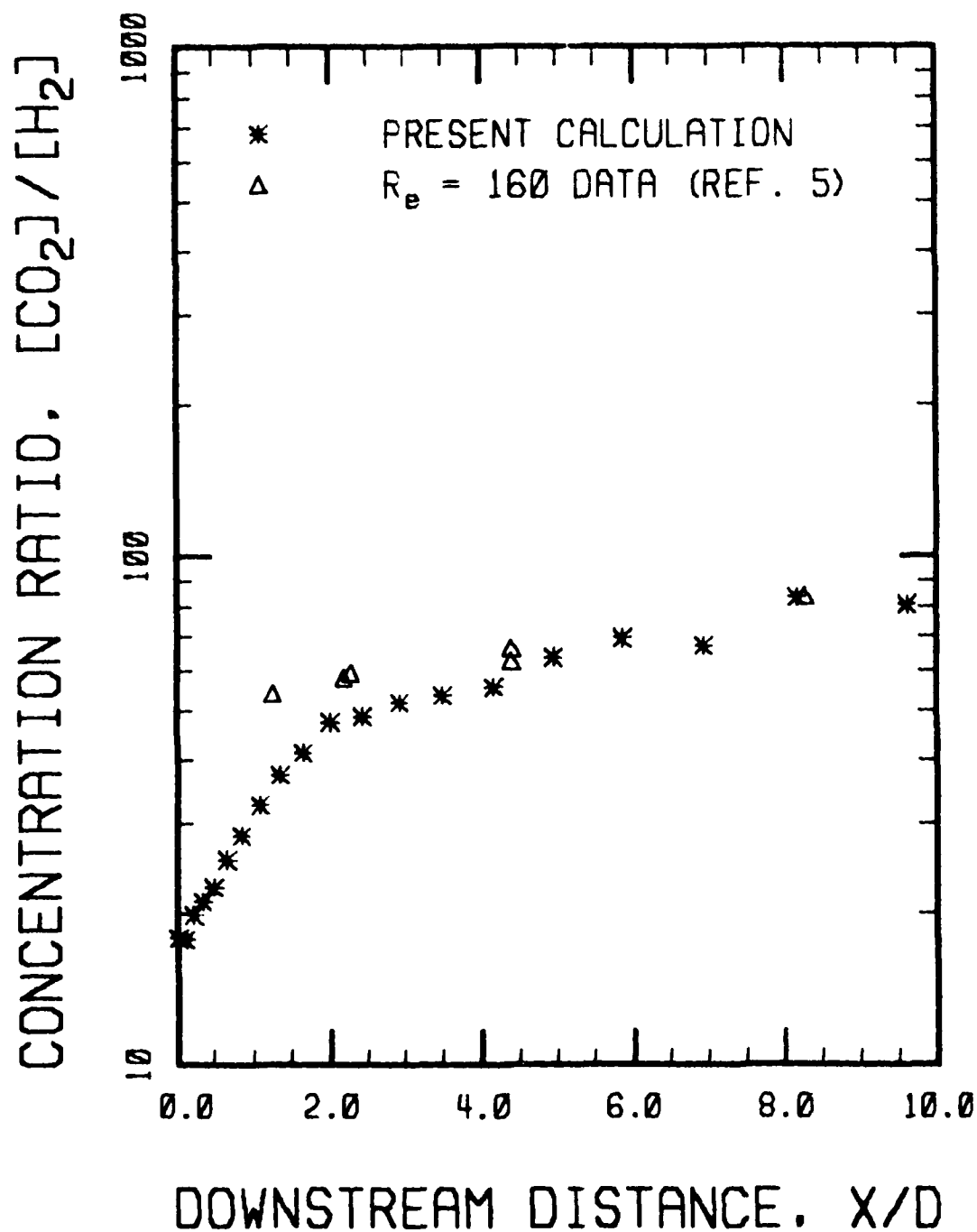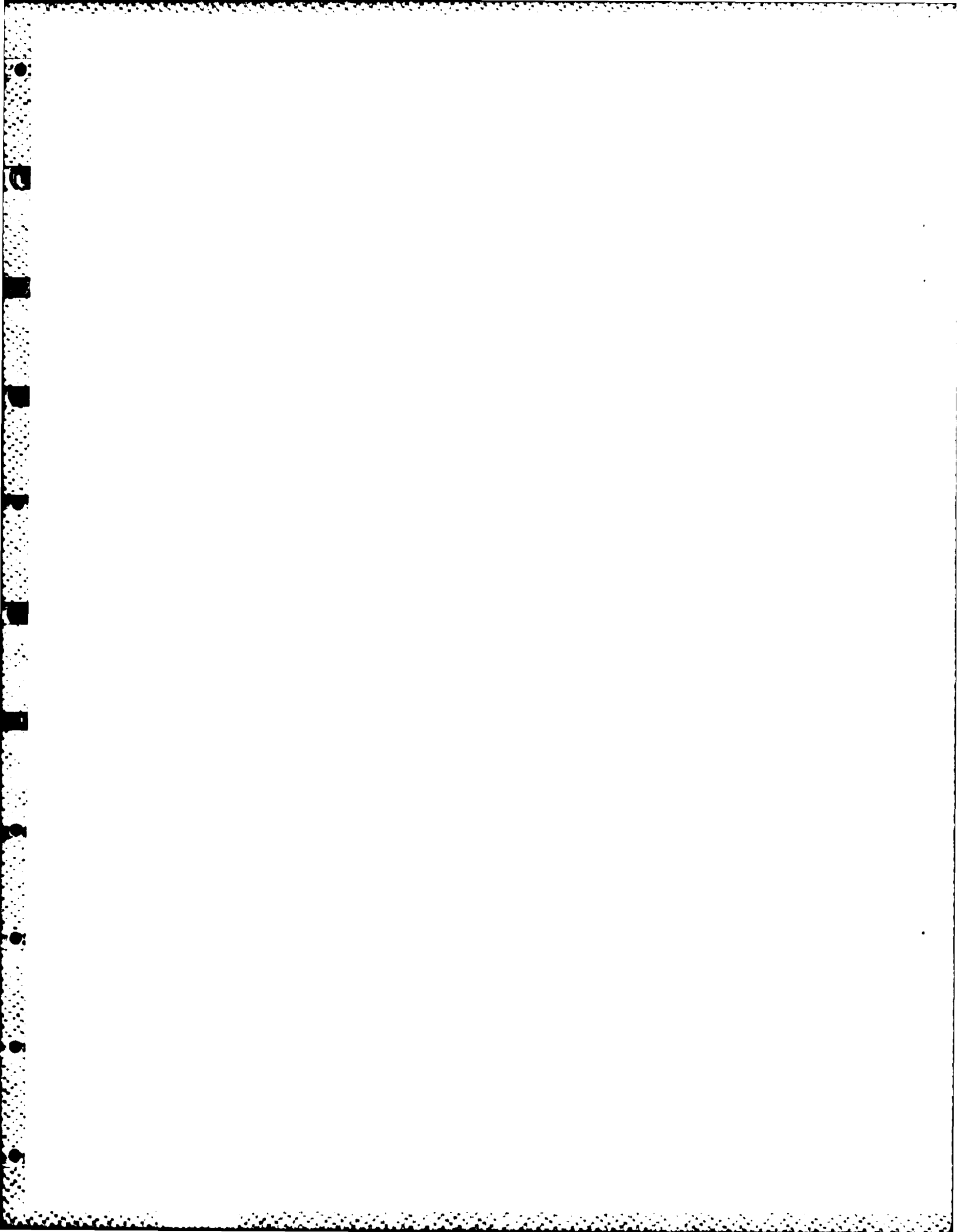
Figure 6. A Comparison of Calculations with Published Data for the Diffusive Separation of H_2 and CO_2 in a Free Jet Expansion From a Sonic Orifice. The orifice is 0.32 cm in diameter, and the stagnation temperature and pressure are 286 K and 1480 dyne/cm^2.

REFERENCES

1. Elgin, J. B., "Monte Carlo Calculations of Mass Spectrometer Flow," Report AFGL-TR-83-0057, Air Force Geophysics Laboratory, February 1983. ADA 128069.

2. Bird, G. A., Molecular Gas Dynamics, Clarendon Press, Oxford, 1976.

3. Abramowitz, M., and Stegun, I. A., Handbook of Mathematical Functions, National Bureau of Standards, 1968, pp. 940,944.

4. Borgnakke, Claus, and Larsen, Paul S., "Statistical Collision Model for Monte Carlo Simulation of Polyatomic Gas Mixture," Journal of Computational Physics, Vol. 18, 1975, pp. 405-420.

5. McCay, T. D., and Price, L. L., "Diffusive separation of binary mixtures of CO_2-H_2 in a sonic-orifice expansion," Physics of Fluids, 26(8), August 1983, pp. 2115-2119.

6. Bird, G. A., "Monte-Carlo Simulation in an Engineering Context," Proceedings of the 12th International Symposium on Rarefied Gas Dynamics, Vol. 74, Progress in Astronautics and Aeronautics, AIAA, New York, 1981.

END

FILMED

8